

Modelling nonlinear optical effects in guest-host systems

Hans Ågren, Yaoquan Tu, and Yi Luo

Theoretical Chemistry, Royal Institute of Technology, Alba Nova University Center, S — 10691 Stockholm, Sweden

We briefly outline a modelling strategy, combining quantum chemistry and molecular dynamics simulations, for obtaining macroscopic nonlinear optical coefficients in guest-host systems like chromophores in solutions or in polymer matrices. The parameters required for the calculation of the macroscopic nonlinear optical property, like the chromophore number density, local field factors, and the order parameter of the chromophore molecules, are derived. These parameters, together with the molecular first hyperpolarizabilities, obtained from quantum chemistry calculations, are used to estimate the macroscopic electro-optic coefficients. The combined approach leads to some new conclusions about the relation of the chromophore property and its solvent interactions in order to optimize the nonlinear optical coefficient. For instance, from the simulation results a totally different notion is derived about the collective properties of octupolar molecules. We find that such molecules receive a solvent induced dipole moment that makes it possible to pole them by an external electric field, but also that they can aggregate as an effect of this solvent interaction.

OCIS codes: 190.0190, 190.4710.

When an electromagnetic field is applied to a material, the interaction between the applied field and the electrons in the material causes a redistribution of the electrons, affecting the transit of the electromagnetic field through it. The consequence is changes of the phase, frequency, or other properties of the applied electromagnetic field. Such phenomena lie behind what is known as nonlinear optical (NLO) properties of a material. Materials with large NLO response have many important applications in photonics^[1]. For example, they can be used to make optical data storage media, optical switches, and electro-optic modulators.

In the field of NLO, organic materials based on the assembly of organic chromophore molecules with highly polarizable π electrons have great potential^[1,2]. Such "molecular materials" are increasingly being recognized as the materials of the future because their molecular nature combined with the versatility of synthetic chemistry can be exploited to optimize the NLO response. Compared with those made of traditional inorganic or semiconductor NLO materials, devices made of organic NLO materials are believed to have several significant advantages: large NLO responses, ultrafast response times, exceptional bandwidth, and dramatically lower operating voltages. Currently, there are basically two types of organic NLO materials being studied: organic NLO crystals containing NLO molecular chromophores and polymeric NLO materials obtained by doping amorphous polymers with NLO molecular chromophores. The latter is more attracting because of reasonable cost in manufacture, higher thermal and chemical stabilities, and high flexibilities being integrated into an optical circuit or fabricated onto many substrates, such as semiconductor electronics.

The NLO response of an organic bulk material is governed by the first hyperpolarizabilities of the constituent molecular chromophores. Experimental studies of first chromophore hyperpolarizabilities involve the synthesis of the chromophore and the measurement of its optical nonlinearities either in the isolated state or in a medium, or both. Such experiments are highly laborious, expensive, and facilities intensive. Therefore, theoretical modelling, including how to design an organic chromophore

with large first hyperpolarizabilities, to model the effects caused by the environment, and to predict the overall NLO response of a material, is of great importance in exploring organic NLO materials.

Taking advantage of the development in modelling of structure-function relationships, many organic chromophores with large NLO responses can now be designed^[3,4]. Quantum chemistry methods, especially those from density-functional theory (DFT), are now widely used as a standard tool in modelling the optical nonlinearities of a chromophore molecule. For an organic NLO crystal or a two-dimensional (2D) film with full periodicity, it is also possible to use quantum chemistry methods to calculate the NLO responses of a chromophore with the effects from the surrounding atoms involved. For the studies of the NLO response of a polymeric material, the Onsager cavity model in which a chromophore molecule occupies a cavity and its surrounding simply being approximated as a dielectric continuum, provides practically the only choices to model a chromophore in a polymer^[5]. Quantum chemistry calculations can be carried out for the chromophore molecule placed in the cavity. The local field factors which reflect the interactions between a chromophore with its surroundings can also be determined. The properties thus derived, however, depend very much on the choices of the shape of the cavity and the dielectric constant of the surrounding continuum. This often makes it difficult to apply the model to the estimation of macroscopic optical nonlinearities.

It follows from the brief survey above, that studies of NLO response of polymeric materials present a great challenge in the theoretical community. New concepts and methods must be used. The recent rapid development in computer simulation techniques has provided an alternative way to study the properties of an interaction system. By using such techniques, especially those of molecular dynamics (MD) simulations, one can estimate the macroscopic properties of a system and study the microscopic origin behind them. Computer simulations have been widely used in the study of solutions, materials, biological systems, and chemical reactions as important complementary tools to experiments. Applica-

tions of MD simulation techniques to the study of NLO molecules in organic solutions and polymers have also been reported^[6-8]. The properties studied are mainly related to, for instance, theoretical predictions of the first hyperpolarizabilities of azobenzene dendrimers in chloroform, and the electric field poling effects of NLO molecules in polymers.

Applications of MD simulations to studies of organic NLO materials are still very limited. Nevertheless, they have shed light on MD simulation techniques as a powerful tool in the study of polymeric NLO materials. As a preliminary study of the NLO properties of such materials, we have recently also carried out series of MD simulations to study the properties of some chromophore molecules in chloroform^[9,10]. Following, we briefly outline the theoretical approaches used and some results obtained from our studies.

The main tool of our choice is the MD simulation technique. The intra- and inter-molecular interactions are modelled by a class I molecular mechanical force field with the parameters required taken from general amber force field (GAFF)^[11,12]. Restrained electrostatic potential (RESP) derived partial atomic charges^[13] are used to model the intra- and inter-molecular non-bond Coulomb interactions. They are obtained by fitting the electrostatic potential from Hartree-Fock 6-31G* calculations of the chromophore molecules and chloroform (CHCl₃) molecules with the geometries fixed to those optimized from the DFT level of theory with B3LYP exchange-correlation functional and 6-31G* basis set. RESP charges can reproduce accurately the dipole moment of a molecule, thus they can also be used in modelling the interactions between the chromophore dipole moment and the external electric field.

The study of the electric field poling effects on the chromophore molecules and the intermolecular interactions are mainly based on the analysis of the chromophore order parameters $\langle \cos \theta \rangle$ and $\langle \cos^3 \theta \rangle$ (where θ is the angle between the molecular dipole moment and the applied electric field) which can be calculated from the MD simulation results. In thermodynamic equilibrium, the order parameters can also be derived from the Boltzmann distribution. If we denote

$$x = \frac{\mu f_z(0) E_p}{kT}, \tag{1}$$

then

$$\langle \cos \theta \rangle = \frac{e^x + e^{-x}}{e^x - e^{-x}} - \frac{1}{x} = L_1(x), \tag{2}$$

and

$$\langle \cos^3 \theta \rangle = \left(1 + \frac{6}{x^2}\right) L_1(x) - \frac{2}{x} = L_3(x), \tag{3}$$

where μ is the molecular dipole moment. E_p is the applied poling field and $f_z(0)$ the local field factor. k and T represent the Boltzmann constant and the absolute temperature, respectively. $L_1(x)$ and $L_3(x)$ are odd-order Langevin functions. In equilibrium, the distribution of $\langle \cos \theta \rangle$, $P(\cos \theta)$ can be evaluated as

$$P(\cos \theta) = \frac{e^{x \cos \theta}}{\int_0^\pi e^{x \cos \theta} \sin \theta d\theta} = \frac{e^{x \cos \theta}}{e^x - e^{-x}}. \tag{4}$$

Therefore, by comparing the order parameters as well as their distributions obtained from MD simulations with those derived from the Boltzmann distributions, we can derive the local field factor $f_z(0)$ and obtain some insight into the intermolecular interactions.

For dipolar chromophore solutions, we also devised an approach to evaluate their macroscopic electro-optic activities. For such solutions, the following formula can be used to estimate the macroscopic second order nonlinear optical susceptibility, $\chi_{zzz}^{(2)}$, and electro-optic coefficient, r_{33} , which are given by^[1]

$$\chi_{zzz}^{(2)} = N [f_z(\omega)]^2 f_z(0) \beta \langle \cos^3 \theta \rangle, \tag{5}$$

and

$$r_{33} = -2\chi_{zzz}^{(2)}/n_z^4, \tag{6}$$

respectively, where N is the chromophore number density (molecules·cm⁻³). ω is the angular frequency and $f_z(\omega)$ the frequency dependent local field factor. β represents the first hyperpolarizability of the chromophore. n_z is the index of refraction. Here, β value can be calculated from quantum chemistry and the quantity N can be derived directly from MD simulations and $f_z(0)$ indirectly from Eq. (2) or Eq. (4). We can therefore focus on how to derive $f_z(\omega)$. We assume that the $f_z(\omega)$ satisfy the Onsager local field function given by^[5]

$$f_z(\omega) = \frac{\epsilon(L_a \epsilon_\infty + 1 - L_a)}{\epsilon(1 - L_a) + L_a \epsilon_\infty}, \tag{7}$$

where ϵ and ϵ_∞ are dielectric constants and L_a is the cavity parameter related to the shape of the chromophore molecule. We thus obtain the local field factors $f_z(0)$ and $f_z(\omega)$ as

$$f_z(0) = L_a(\epsilon - 1) + 1, \tag{8}$$

$$f_z(\omega) = L_a(\epsilon_\infty - 1) + 1, \tag{9}$$

with

$$\epsilon_\infty = n_z^2. \tag{10}$$

For many solutions with organic solvents, the index of refraction is about 1.4-1.5^[14]. As a reasonable approximation, the index of refraction of CHCl₃ ($n = 1.446$)^[14] is used throughout in this work. In finding $f_z(\omega)$, we assumed the L_a parameter appearing in Eq. (9) to be the same as that in Eq. (8). Therefore, we obtain L_a as

$$L_a = \frac{f_z(0) - 1}{\epsilon - 1}. \tag{11}$$

Here, $f_z(0)$ is derived from MD simulation results and the dielectric constant of CHCl₃ ($\epsilon = 4.806$)^[14] has been used.

Octupolar molecules are generally believed to be of potential use in developing nonlinear optical materials because they do not easily form molecular aggregates^[15].

This often put against the conjectured drawback that electric fields have no poling, or ordering, effect for this class of molecules due to the lack of a permanent ground state dipole moment. We have put forward the notion that for an octupolar molecule in solution, the thermal motions of the atoms as well as the intermolecular interactions, will, under normal conditions, induce molecular dipole moments, and explore the consequence of this notion for the poling capability. Studies on a prototypical octupolar molecule were reported in Ref. [9], namely 1,3,5-triamino-2,4,6-trinitrobenzene (TATB, see Fig. 1 for the chemical structure) molecules dissolved in CHCl_3 and the electric field poling effects on TATB molecules in this solution. Three solutions, each containing 512 CHCl_3 molecules as solvent and 64, 80, and 96 TATB molecules as solutes in the simulation box, labelled as solutions 1, 2, and 3, respectively, were simulated. A NPT ensemble with $P = 1$ atm and $T = 300$ K is used in the simulations.

Figure 2 shows the evolution of the average TATB dipole moments in solution 1, calculated using partial atomic charges without the external electric field after an initial simulation of 2 ns. The average molecular dipole moment after applying an external poling field with a strength of 2.0 V/nm is also shown in the same figure. The evolution of dipole moments of the TATB molecules in solutions 2 and 3 are rather similar to that in solution 1. From the figure we can see that even though TATB has no dipole moment at equilibrium geometry, it does have significant dipole moment in solutions. The dipole moment origins in the thermal motions of the atoms and from intermolecular interactions. By

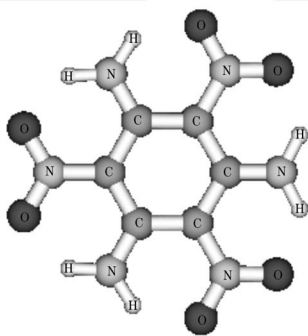


Fig. 1. The chemical structure of TATB molecule.

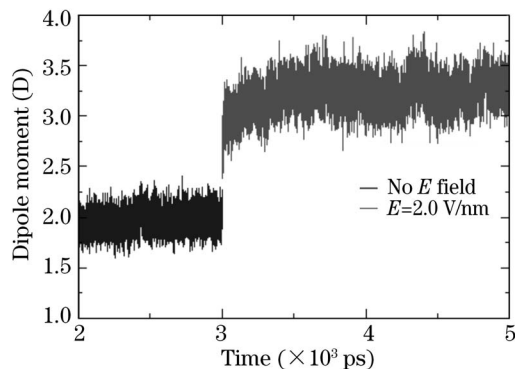


Fig. 2. Evolution of the average TATB dipole moment in solution 1. An external electric field of 2 V/nm is applied after 3 ns.

applying an external electric field, the TATB dipole moments increase significantly. We attribute the increases of the TATB dipole moment to additional deformations of the TATB molecular structure that occurred after applying an external electric field.

The non-zero TATB dipole moments indicate that there would exist electric field poling effects on the TATB molecules in solutions. The MD simulation results show that this indeed is the case. In Fig. 3 we show the evolution of the order parameter $\langle \cos \theta \rangle$ of TATB molecules in solution 1. Without the external electric field, $\langle \cos \theta \rangle$ is close to 0 because the molecular dipole moments are randomly oriented. From the figure, we find that $\langle \cos \theta \rangle$ increases significantly shortly after the electric field is applied. The very short response time of the order parameter $\langle \cos \theta \rangle$ upon the applied electric field indicates that the change of the order parameters is most probably due to the vibrational motions of the atoms which result in the reorientation of the TATB molecular dipole moments and it is unlikely that such a change is caused by the rotational motions of the TATB molecules.

Table 1 lists the calculated $\langle \cos \theta \rangle$ and $\langle \cos^3 \theta \rangle$ quantities for three solutions in equilibrium from the MD simulations averaged at the time interval 4–5 ns. In the same table, we also list the theoretically estimated local field factors for the three solutions that are obtained by reproducing the theoretical order parameters $L_1(x)$ and $L_3(x)$ to $\langle \cos \theta \rangle$ and $\langle \cos^3 \theta \rangle$, respectively. In the calculations of $L_1(x)$ and $L_3(x)$, ensemble averaged equilibrium dipole moments are used. The resulting $L_1(x)$ and $L_3(x)$ quantities are also listed in Table 1. We can see that the order parameters for the TATB molecules in the three solutions are very close to one another and the order parameters $L_1(x)$ and $L_3(x)$ derived using the effective electric fields are in good agreement with those from the MD simulations.

In order to further understand the nature of the intermolecular interactions in the simulated solutions, a snapshot for the configuration of solution 1 is taken at 5 ns in the presence of an applied electric field of 2 V/nm with the solvent molecules (CHCl_3) excluded, as shown in Fig. 4. We also find clearly that TATB molecules tend to aggregate and both the solvent and the applied external field are still unable to break up the aggregates. After a careful investigation of the molecular

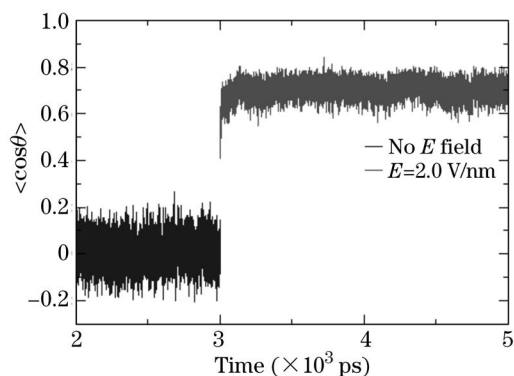


Fig. 3. Evolution of the average TATB order parameter $\langle \cos \theta \rangle$ in solution 1. An external electric field of 2 V/nm is applied after 3 ns.

Table 1. Order Parameters $\langle \cos\theta \rangle$ and $\langle \cos^3\theta \rangle$ Calculated from MD Simulations, the Estimated Local Field Factor $f_z(0)$ and the Corresponding Theoretical Order Parameters $L_1(x)$ and $L_3(x)$

	Solution 1	Solution 2	Solution 3
$\langle \cos\theta \rangle$	0.71 ± 0.31	0.73 ± 0.29	0.72 ± 0.31
$\langle \cos^3\theta \rangle$	0.50 ± 0.33	0.52 ± 0.32	0.52 ± 0.33
$f_z(0)$	0.66	0.70	0.63
$L_1(x)$	0.71	0.73	0.73
$L_3(x)$	0.49	0.51	0.51

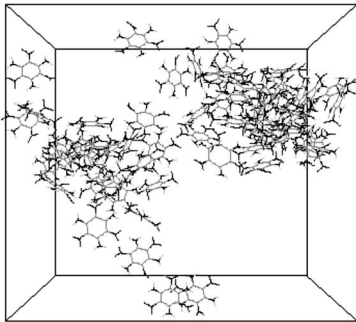


Fig. 4. The structure of solution 1. The snapshot is taken at 5 ns with an external electric field of 2 V/nm applied. The electric field is parallel to the plane of the figure with the direction from the left to the right. The simulation box contains 64 TATB molecules and 512 CHCl_3 molecules, respectively. The solvent (512 CHCl_3 molecules) is not shown.

configuration shown in Fig. 4, we find that there exist strong intermolecular hydrogen-bonding interactions between the H atoms in the amine group ($-\text{NH}_2$) and the O atoms in the nitro group ($-\text{NO}_2$) and that it is the strong intermolecular hydrogen-bonding interactions which are responsible for the aggregation of the TATB molecules and the attenuation of the applied external electric fields. Due to the strong hydrogen-bonding interactions, the applied electric field has little effect on the orientations of the TATB molecules although significant effects of the electric fields on the molecular dipole moments are observed.

In the following section, we report the use of MD simulation techniques to study properties related to the macroscopic electro-optic activities of NLO materials. We focus on the electric field poling effects on the dipolar chromophores and on how to use computer simulations to derive some parameters required for the calculation of macroscopic NLO properties, namely the chromophore number density, local field factors, and order parameters for the chromophores. The obtained parameters, together with the molecular first hyperpolarizabilities obtained from quantum chemistry calculations, are used to estimate the macroscopic electro-optic coefficient. MD simulations are carried out for an ensemble of typical NLO dipolar molecules, namely dispersed red (4,4'-dimethylaminonitroazobenzene, DR, see Fig. 5), dissolved in CHCl_3 . Six solutions, each containing 512 CHCl_3 molecules as solvent and 16, 32, 48, 64, 80, 96 DR molecules, respectively, as solutes in the simulation box, were studied (labelled as solutions 1, 2, 3, 4, 5, and 6,

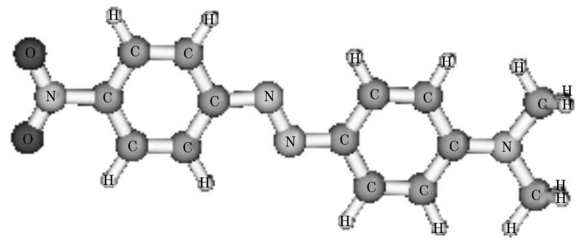


Fig. 5. Structure of DR molecule.

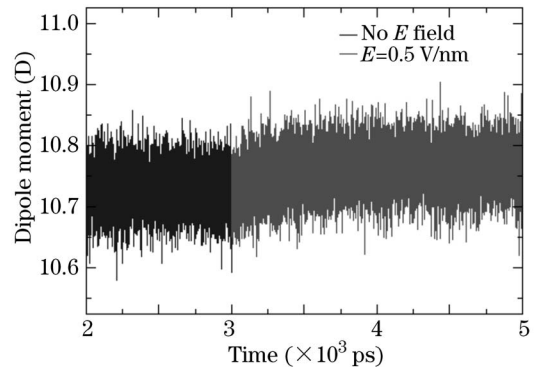


Fig. 6. Evolution of the average DR dipole moment in solution 4. An external electric field of 0.50 V/nm is applied after 3 ns.

respectively). A NPT ensemble is used in the simulations with $P = 1$ atm, and $T = 300$ K.

Figure 6 shows the evolution of the average DR dipole moment in solution 4, calculated using partial atomic charges without the external electric field (2–3 ns) and with an external poling field of 0.50 V/nm applied (3–5 ns) after an initial simulation of 2 ns. From the figure we can see that the dipole moment of the DR monomer in chloroform fluctuates around 10.7–10.8 D and the applied poling field has only a slight effect on it. The evolution of the dipole moments of the DR molecules in other solutions are rather similar to that in solution 4.

In Fig. 7 we show the evolution of the order parameter $\langle \cos\theta \rangle$ of DR molecules in solution 4. Without the external electric field, $\langle \cos\theta \rangle$ fluctuates around 0 because the molecular dipole moments are randomly oriented. By applying a poling field, $\langle \cos\theta \rangle$ increases gradually. It takes nearly 0.5 ns for $\langle \cos\theta \rangle$ to reach a stable value around 0.8. Because the applied field has little effect on the magnitude of the monomer dipole moment, we attribute the change of $\langle \cos\theta \rangle$ to the rotational motions of DR molecules which make the chromophore dipole moments reorientate along the field applied. The electric field poling effects on the DR molecules can also be seen from Fig. 8. In the figure, we show a snapshot for the configuration of the 64 DR molecules in solution 4 taken at 5 ns in the presence of an applied electric field of 0.5 V/nm. The electric field is parallel to the plane of the figure with the direction from left to right. For clarity, the 512 CHCl_3 molecules in the simulation box are not shown. We can see from the figure that DR molecules show ordered orientations with the molecular dipole moments more or less along the applied

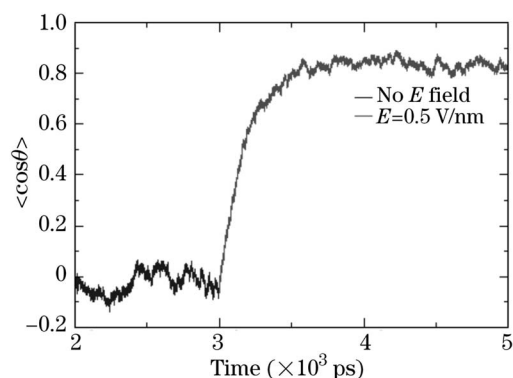


Fig. 7. Evolution of the average DR order parameter $\langle \cos\theta \rangle$ in solution 4. An external electric field of 0.50 V/nm is applied after 3 ns.

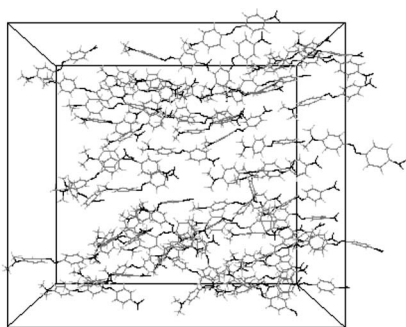


Fig. 8. The configuration of DR molecules in solution 4. The snapshot is taken at 5 ns with an externally applied electric field of 0.5 V/nm. The electric field is parallel to the plane of the figure with the direction from left to right. The simulation box contains 64 DR molecules and 512 CHCl_3 molecules, respectively. The solvent CHCl_3 molecules are not shown.

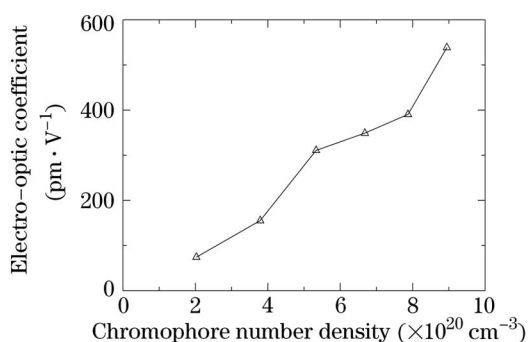


Fig. 9. Calculated variation of electro-optic coefficient r_{33} with chromophore number density N .

electric field. We can also find that no aggregation of DR molecules occurs in the solution, showing that DR molecules are well solvated in chloroform.

The order parameters $\langle \cos\theta \rangle$ and $\langle \cos^3\theta \rangle$ for the DR chromophores in the six solutions averaged at the time interval of 4–5 ns are listed in Table 2. The corresponding local field factors $f_z(0)$ which are obtained by fitting the $\langle \cos\theta \rangle$ values with the Langevin functions $L_1(x)$ also are listed. In the calculation of the x value in $L_1(x)$, the averaged chromophore dipole moment is used. We also listed the cavity parameter L_a for the chromophore molecules and the frequency dependent local field factor $f_z(\omega)$. They are calculated according to Eqs. (11) and (9), respectively. It is clear that the L_a value varies from 0.053 to 0.130, much less than that for a spherical cavity (0.333). This indicates that the chromophore molecules correspond to prolate spheroid cavities, in agreement with the fact that the shape of the DR molecules studied in this work is far from the spherical one.

Table 2. The Calculated Order Parameters $\langle \cos\theta \rangle$, $\langle \cos^3\theta \rangle$, the Local Field Factors $f_z(0)$, $f_z(\omega)$, and the Cavity Parameter L_a

Solution	$\langle \cos\theta \rangle$	$\langle \cos^3\theta \rangle$	$f_z(0)$	$f_z(\omega)$	L_a
1	0.807 ± 0.186	0.597 ± 0.278	1.200	1.057	0.0525
2	0.818 ± 0.172	0.612 ± 0.274	1.264	1.076	0.0694
3	0.844 ± 0.179	0.670 ± 0.269	1.474	1.136	0.1245
4	0.836 ± 0.177	0.651 ± 0.274	1.407	1.117	0.1069
5	0.832 ± 0.187	0.647 ± 0.273	1.371	1.106	0.0975
6	0.846 ± 0.200	0.675 ± 0.269	1.496	1.142	0.1303

Table 3. Calculated Density $\langle \rho \rangle$, Chromophore Number Density N , Macroscopic Second Order NLO Susceptibility $\chi_{zzz}^{(2)}$, and Electro-Optic Coefficient r_{33}

Solution	$\langle \rho \rangle$ ($\text{g} \cdot \text{cm}^{-3}$)	N ($\times 10^{20} \text{ cm}^{-3}$)	$\chi_{zzz}^{(2)}$ ($\text{pm} \cdot \text{V}^{-1} \text{esu}$)	r_{33} ($\text{pm} \cdot \text{V}^{-1} \text{esu}$)
1	1.377 ± 0.005	2.027	-162.1	74.2
2	1.372 ± 0.005	3.790	-339.2	155.2
3	1.367 ± 0.005	5.333	-679.3	310.7
4	1.359 ± 0.004	6.680	-762.9	349.0
5	1.352 ± 0.004	7.872	-853.6	390.5
6	1.347 ± 0.004	8.944	-1171.1	538.5

The calculated density $\langle \rho \rangle$ of the solutions, and the corresponding number density N of the chromophores, the macroscopic NLO susceptibility $\chi_{zzz}^{(2)}$, and electro-optic coefficient r_{33} , calculated according to Eqs. (5) and (6), respectively, are listed in Table 3. In the calculation of $\chi_{zzz}^{(2)}$, the β value of a gas state chromophore is determined from DFT calculations with the DALTON^[16] program. At the “best” functional level (CAMB3LYP) and 6-31G* basis set, the β value along the molecular dipole moment at a wavelength of $\lambda = 1.9 \mu\text{m}$ is calculated to be 1.157×10^4 a.u., corresponding to 99.94×10^{-30} esu^[17]. From Table 3, we find that the magnitudes of the calculated macroscopic NLO properties increase significantly with the loading. In Fig. 9 we show the variation of r_{33} with chromophore number density N calculated from this work. We can also see that the electro-optic coefficient increases with the chromophore number density. The experimentally observed maximum of the electro-optic coefficient for polymers containing chromophores characterized by large dipole moments and polarizabilities^[18] is not found in this study. The possible reason is that the loading in this study is not so high that there is no strong interactions between the chromophores. We will in the coming work study this phenomenon more closely.

H. Ågren's e-mail address is agren@theochem.kth.se.

References

1. L. R. Dalton, W. H. Steier, B. H. Robinson, C. Zhang, A. Ren, S. Garner, A. Chen, T. Londergan, L. Irwin, B. Carlson, L. Fifield, G. Phelan, C. Kincaid, J. Amend, and A. Jen, *J. Mater. Chem.* **9**, 1905 (1999).
2. L. Dalton, A. Harper, A. Ren, F. Wang, G. Todorova, J. Chen, C. Zhang, and M. Lee, *Ind. Eng. Chem. Res.* **38**, 8 (1999).
3. S. R. Marder, C. B. Gorman, F. Meyers, J. W. Perry, G. Bourhill, J.-L. Bredas, and B. M. Pierce, *Science* **265**, 632 (1994).
4. A. K.-Y. Jen, Y. Cai, P. V. Bedworth, and S. R. Marder, *Adv. Mater.* **9**, 132 (1997).
5. D. M. Burland, R. D. Miller, and C. A. Walsh, *Chem. Rev.* **94**, 31 (1994).
6. W.-K. Kim and L. M. Hayden, *J. Chem. Phys.* **111**, 5212 (1999).
7. M. Makowska-Janusik, H. Reis, M. G. Papadopoulos, I. G. Economou, and N. Zacharopoulos, *J. Phys. Chem. B* **108**, 588 (2004).
8. Y. Yamaguchi, Y. Yokomichi, S. Yokoyama, and S. Mashiko, *Theo. Chem.* **545**, 187 (2001).
9. Y. Tu, Y. Luo, and H. Ågren, Can octupolar molecules be poled by an external electric field? (submitted).
10. Y. Tu, Y. Luo, and H. Ågren, Theoretical study of electro-optic activity of dipolar chromophore solutions (submitted).
11. J. Wang, R. M. Wolf, J. W. Caldwell, P. A. Kollman, and D. A. Case, *J. Comput. Chem.* **25**, 1157 (2004).
12. J. Wang, R. M. Wolf, J. W. Caldwell, P. A. Kollman, and D. A. Case, *J. Comput. Chem.* **26**, 114 (2005).
13. C. I. Bayly, P. Cieplak, W. D. Cornell, and P. A. Kollman, *J. Phys. Chem.* **97**, 10269 (1993).
14. D. R. Lide, *CRC Handbook of Chemistry and Physics* (73rd edn.) (CRC Press, 1992).
15. J. Zyss and I. Ledoux, *Chem. Rev.* **94**, 77 (1994).
16. DALTON, Release 2.0, <http://www.kjemi.uio.no/software/dalton/dalton.html> (2005).
17. Y. Wang, L. Frediani, P. Salek, and H. Ågren, (to be published).
18. L. R. Dalton, A. W. Harper, and B. H. Robinson, *Proc. Natl. Acad. Sci.* **94**, 4842 (1997).